INSTITUTE OF PHYSICS PUBLISHING JOURNAL OF PHYSICS B: ATOMIC, MOLECULAR AND OPTICAL PHYSICS

J. Phys. B: At. Mol. Opt. Phys. **39** (2006) 1605–1623 doi:10.1088/0953-4075/39/7/005

Ridged atomic mirrors and atomic nanoscope

D Kouznetsov[1], H Oberst[1], A Neumann[2], Y Kuznetsova[2], K Shimizu[1], J-F Bisson[1], K Ueda[1] and S R J Brueck[2]

[1] Institute for Laser Science, University of Electro-Communications, 1-5-1 Chofugaoka, Chofu, Tokyo 182-8585, Japan
[2] Center for High Technology Materials, University of New Mexico, 1313 Goddard SE, Albuquerque, NM 87106-4343, USA

E-mail: dima@ils.uec.ac.jp

Received 2 December 2005
Published 13 March 2006
Online at stacks.iop.org/JPhysB/39/1605

Abstract

Recent results on the reflection of waves from ridged mirrors are discussed. Numerical calculations, analytical estimates and the direct measurements of coefficient of specular reflection of atomic waves from solid-state mirrors are combined. The reflectivity is approximated as an elementary function of period L of ridges, their width ℓ, wavenumber K, grazing angle θ and effective depth w of the van der Waals potential. In a special case $L = \ell$, the fit reproduces the reflectivity of flat surfaces. Our approximation allows us to optimize the L at given ℓ and estimate the maximum performance of a ridged mirror. Such a mirror is suggested as a focusing element for the nano-scale imaging system.

1. Introduction

In the last century, new methods appeared in addition to conventional optical microscopy. Electron microscopy and various kinds of near-field microscopy (tunnelling microscopy, atomic force microscopy, capacitance microscopy) were successfully developed and applied. The use of atoms as a probe was also considered [1, 2]. The atomic microscope could provide long depth of view and high resolution (like an electron microscope) and be completely non-destructive, due to the low energy of thermal-speed atoms. For example, at 4 K temperature, the He atoms may have a speed $V = 100\,\mathrm{m\,s^{-1}}$ and wavenumber $K = MV/\hbar = 6.3\,\mathrm{nm^{-1}}$. In principle, with a microscope, one could see the structure of individual molecules without destroying them.

There has been certain progress in the manipulation of atoms, using narrow localization of light fields [3], evanescent optical wave [4–6] or static electric or magnetic fields [7–10]. The focusing of atomic beam with a concave mirror [11], as well as with a Fresnel atomic lens [12], is achieved; atom interferometry [13] and atom holography [14] are demonstrated. In the background of these achievements, the atom microscopy remains rather a challenging

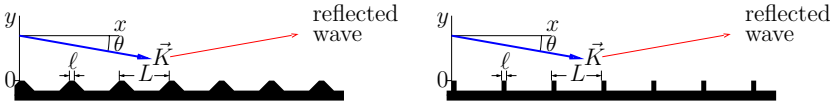

Figure 1. Wave with wavevector $\vec{K}$ incident at the grazing angle θ onto the surface with a grating structure. (a) Structure with trapezoidal ridges [18]; (b) structure with rectangular ridges [19].

experiment than a useful tool. The main problem of realization of an atomic microscope is the precise focusing of the atomic beam. Such precision could be provided by the solid-state focusing element.

There is no material transparent for the low-energy atomic beam. The possible solution for the atomic focusing element could be the solid-state mirror. The attractive character of the atom–surface interaction is the main mechanism which limits the performance of the solid-state mirrors. The van der Waals interaction (WVI) prevents the efficient reflection. This interaction becomes repulsive only at small distances when the atoms feel the discrete character of the material of the mirror, which leads to the diffuse scattering. The quantum reflection (QR) [11, 15–17] can be efficient, if the normal component of the atom wavevector is small. This limits the use of the solid-state atomic mirrors to very cold atoms [15] and/or small values of the grazing angle [16, 17]. The numerical aperture (NA) of the collimated beam should be small, even if atoms are cooled in a magneto-optical trap (MOT) [16, 17].

The enhancement of the working range of the grazing angle is necessary for the practical application of the atom mirrors. Certain achievements in such enhancement are related to the so-called ridged mirrors [18, 19]. The simplified view of such a mirror is shown in figure 1. The idea of a ridged mirror is to reduce the effective constant C_4 of the VWI. At the grazing incidence, atoms feel only the top of the ridges, and structures with trapezoidal ridges (figure 1(a)) show reflectivity (reflection coefficient) similar to that of a structure with rectangular ridges (figure 1(b)); only the period L ridges and their width ℓ are important.

To improve the performance of the solid-state atomic mirrors, the estimate of reflectivity is required. Several estimates were already published. First, the reflectivity of a ridged surface was suggested to be that of the plane surface with constant C_4 scaled with factor ℓ/L. Such an estimate, let us denote it as R_s, did not agree with the first experiments on the reflection of excited Ne and He atoms on ridged surfaces reported in [18, 19].

A completely different estimate is based on the concept of the Zeno effect. At large values of L, and small values of the grazing angle θ, the ridges act as idealized absorbers, which just block the part of the wavefront of the atomic wave. In this case, the x-coordinate (figure 1) plays the role of time, and the ridges can be interpreted as detectors which entangle the state of the atomic wavefunction with many other degrees of freedom. With such entanglement, the measurement of the position of the atom could be performed without any additional distortion of state of atom. The frequent measurement of the y-coordinate of an atom prohibits the transition from the half-space $y > 0$ to the half-space $y < 0$, due to the spatial Zeno effect [20]. The frequency of such 'measurements' $f = V/L$, where V is the velocity of the atom. The frequency of the atomic wavefunction related to the movement of the particle in the y-direction is $\omega = Mv^2/(2\hbar)$, where M is the mass of the atom and $v = V\sin\theta = Vs \approx V\theta$ is the normal component of the velocity. In the practical case, $\theta \ll 1$ and we can replace $s = \sin\theta$ by θ. At $f > \omega$, we expect significant reflection due to the Zeno effect. The assumption that the detection of atoms in the half-space with frequency f is equivalent to the continuous absorption with the same frequency leads to the Zeno estimate [20] of the

reflectivity:

$$R_{\mathrm{Z}} = R_{\mathrm{Z}}(p) = \frac{\sqrt{\sqrt{1+1/p^4}+1}-\sqrt{2}}{\sqrt{\sqrt{1+1/p^4}+1}+\sqrt{2}} \approx \exp(-\sqrt{8}p), \tag{1}$$

where

$$p = \sqrt{2f/\omega} = \sqrt{KL}s \tag{2}$$

is the dimensionless transversal momentum; $K = MV/\hbar$ is the wavenumber. At $p \gg 1$, the strong absorption (or diffuse scattering) takes place; while at $p \ll 1$, the specular reflection is strong and the ridged surface is a good mirror.

The same estimate (1) can be obtained from the assumption that the ridged surface behaves as a distributed absorber with absorption length L [21]. This approximation ignores the periodic character of ridges, their width and the VWI of atoms with the surface. Nevertheless, such an estimate agrees with the published experimental data for Ne* [18] and He* [19] atoms reflected from various ridged surfaces. This agreement is better than that for the fit of numerical simulations [21] for the idealized thin ridges ($\ell = 0$, no VWI):

$$R_{\mathrm{o}} = R_{\mathrm{o}}(p) = \exp(-1.68(1+0.018p^2)p). \tag{3}$$

In order to attribute the deviation to the VWI, the correction due to the potential,

$$U(y) = C_4/y^4 \tag{4}$$

is considered [21]. The rough perturbative analysis led to the corrected estimate

$$R_{\mathrm{p}} = R_{\mathrm{o}}(p)\exp\left(-\mathcal{E}\left(\frac{w^2}{2K\ell^3}\right)K\ell\theta\right), \tag{5}$$

where

$$w = \sqrt{2MC_4}/\hbar \tag{6}$$

is the effective depth of the potential, and $\mathcal{E} = \mathcal{E}(z)$ is the solution of the equation

$$\mathcal{E}^4 = (1+\mathcal{E})z. \tag{7}$$

Parameter $\mathcal{E}$ has the sense of the normalized thickness of a boundary layer where the potential destroys the phase of a quasi-classical particle while it passes by the ridge.

The estimate R_{p} showed good agreement with the published experimental data [18, 19, 21], especially for reflection of excited He atoms from surfaces with L of several microns. We wanted to extrapolate the estimate R_{p} by (5) to the case of a ridged mirror with very small L, where this estimate predicted enlargement of the range of working angles. The ridged mirror with sub-micron period L was manufactured at the University of New Mexico (UNM). Such a mirror was expected either to have extended range of values of the grazing angle θ, or to confirm the estimate R_{s} with scaling of the van der Waals constant [18], as it actually did. The measured reflectivity versus the normal component $k = K\sin(\theta) = Ks$ of the wavevector is shown in figure 2 with dots. The perturbative estimate R_{p} lies significantly above the experimental dots, and the estimate R_{s} in [18] with scaling of the van der Waals constant (the dashed line in figure 2) shows much better agreement.

To get the picture of the cross-section of the ridged surface, the sample was cut (intentionally cracked) across the ridges. One half of the initial sample was used for the measurements of the reflectivity; the other half was analyzed with an electron microscope. The resulting images are shown in figures 2(b) and (c).

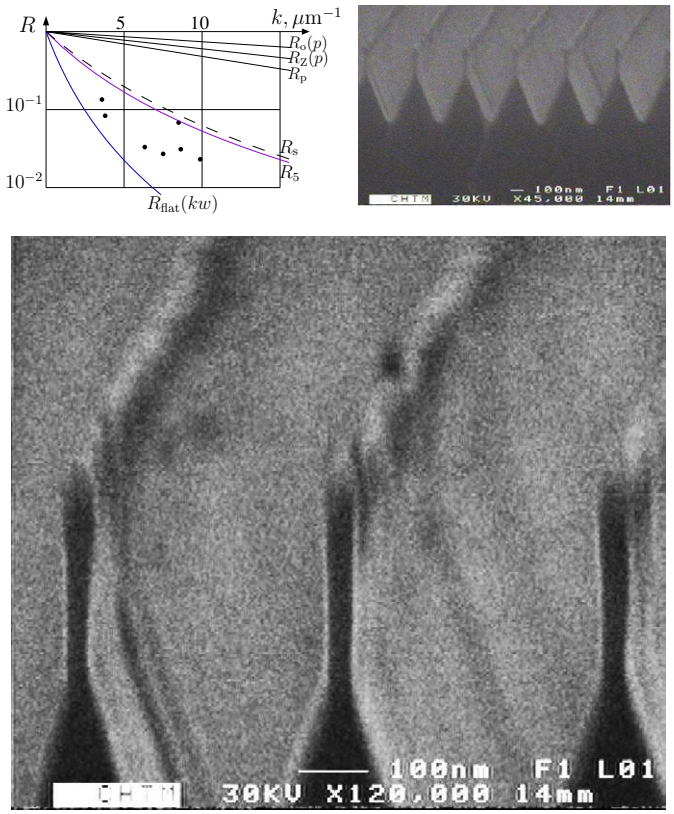

Figure 2. Reflectivity versus transversal wavenumber $k = K\sin(\theta) = Ks$ for the UNM sample and various estimates (left); $L = 400$ nm, $\ell = 40$ nm, $V = 20$ m s^{-1}. The electron microscope image of the cut of the sample (right). The central part of the picture with higher magnification and enhanced contrast (bottom).

The UNM sample is the most dense ridged mirror; those reported in [18, 19] have period L an order of magnitude larger (several micron). Also, the shape of ridges (figures 2(b) and (c)) is very different from trapezoidal [18] and from rectangular [19]; we even doubt if they have a flat-top, the top does not look very regular (figure 2(c)). Nevertheless, we expect the period L and the width ℓ of the ridges remain the most important parameters which determine the performance of such a ridged mirror.

As we reduce L, the estimate R_p begins to fail, and that with scaling of the van der Waals constant [18] becomes valid. For the optimization of ridged mirrors, it would be good to have an estimate similar to R_p at large L (say, several microns) and similar to R_s at sub-micron L. In this paper, we suggest such an estimate. Below, we analyse the asymptotic behaviour of reflectivity as a universal function of $L, \ell, K, s = \sin(\theta)$ and w. We formulate its properties as requirements for the good approximation of the reflectivity. We construct a simple function R_5 by (28) which satisfies these criteria. (In figure 2, this estimate is shown with the solid line, just below the dashed line.) Then we use the function R_5 to estimate the minimal size of a spot where the atoms can be focused with such a mirror, and estimate the flux of atoms in such a system.

2. Reflectivity $R(L, \ell, K, \sin(\theta), w)$

We want a simple approximation for the reflection coefficient R, which allows prediction of properties of ridged atomic mirrors and optimization of their parameters. In this section, we summarize our wishes about behaviour of this function.

In this paper, we neglect the defects of the sample; moreover, we do not take into account the shape of the ridges; we assume that the trapezoidal ridges (figure 1(a)) are as efficient as rectangular (figure 1(b)). We do not consider the height of the ridges, assuming that it is sufficient to neglect reflection from valleys between the ridges. In this approximation, the reflectivity should be determined by the period L, width ℓ, wavenumber K, grazing angle θ and effective depth w of the van der Waals potential. Let the reflectivity be $R = R(L, \ell, K, s, w)$, where $s = \sin(\theta)$.

In practical cases, $\theta \ll 1$, so we make no difference between $\sin(\theta)$ and θ. We keep this sine for the case of comparison of our fit with possible numerical simulations (which are difficult to perform in for realistic ridged atomic mirrors), while the reflectivity begins to drop down at θ of the order of 1 rad.

From the definition of the reflectivity, it is supposed to be a real positive function that does not exceed unity,

$$0 \leqslant R(L, \ell, K, s, w) \leqslant 1, \tag{8}$$

at least at real non-negative values of its arguments.

In principle, some of arguments of the function R have no need to be positive or even real. For example, complex K could be considered; it might describe the reflection of an evanescent wave. Pure imaginary values of w would correspond to the repulsive atom–surface interaction. Also, complex values of w could describe some spontaneous relaxation due to the broken symmetry in the vicinity of the surface: the interaction may allow some transitions which are strictly prohibited in free space. However, in order to deal with analytic function, we would have to consider the complex amplitude of scattering [21, 23]. In this paper, we consider only real non-negative values of L, ℓ, K, s and w; also, we assume, $L \geqslant \ell$. Therefore, we deal with the reflectivity which is the square of modulus of the zeroth-order scattering amplitude.

From the dimensional reasons, at $K > 0$, we can write the reflectivity as

$$R(L, \ell, K, s, w) = R(KL, K\ell, 1, s, Kw). \tag{9}$$

Similarly, for $w > 0$, we could represent the reflectivity as

$$R(L, \ell, K, s, w) = R(L/w, \ell/w, Kw, s, 1), \tag{10}$$

and reduce the number of variables. In this paper, we keep all the five variables; this simplifies the consideration of limiting cases $K = \infty$ and $w = 0$.

Consider extremely dense ridges. When $L = \ell$, the reflectivity should be the same as the reflectivity $R_{\text{flat}} = R_{\text{flat}}(wKs)$ of the flat surface,

$$R(L, L, K, s, w) = R_{\text{flat}}(wKs). \tag{11}$$

Note that the right-hand side of equation (11) does not depend on L. The reflection from the flat surface is considered in [16, 17, 23]. The exponential estimate for the reflectivity was suggested in [23] for the case of small values of $q = wKs$; in our notations, it reads

$$R_{\text{flat}}(q) \approx \exp(-4q). \tag{12}$$

Reducing the wavenumber K or the grazing angle θ, the reflectivity should increase till unity:

$$R(L, \ell, 0, s, w) = R(L, \ell, K, 0, w) = 1. \tag{13}$$

Note that the special case $w = 0$ should allow simulations with methods developed for the scattering of electromagnetic waves at the periodic surfaces [27, 28]; then the surface becomes analogue of a perfect conductor for the tangential polarization of an electromagnetic wave.

As we increase L, K, or w, the reflectivity should decrease down to zero:

$$R(\infty, \ell, K, s, w) = 0, \tag{14}$$

$$R(L, \ell, \infty, s, w) = 0, \tag{15}$$

$$R(L, \ell, K, s, \infty) = 0. \tag{16}$$

The perturbative estimate R_p by (5) can also be considered as the limiting case; at large values of L, and small values of θ, we expect

$$R(L, \ell, K, s, w) \approx R_\mathrm{p}(L, \ell, K, s, w). \tag{17}$$

We assume that R is a smooth function of its arguments; we expect that this assumption is valid at $KL(1 - \cos(\theta)) < 2\pi$, while there are no negative orders of scattering discussed in [21]; for the realistic case we may expect that

$$\partial R(L, \ell, K, s, w)/\partial \ell < 0, \tag{18}$$

$$\partial R(L, \ell, K, s, w)/\partial K < 0, \tag{19}$$

$$\partial R(L, \ell, K, s, w)/\partial s < 0, \tag{20}$$

$$\partial R(L, \ell, K, s, w)/\partial w < 0. \tag{21}$$

We specify the 'realistic case' for conditions (18)–(21), because at very small w and large L, the reflection from top of the ridges may dominate. Then condition (18) may be broken. In this case, the flat surface ($\ell = L$) would provide better reflectivity than a set of ridges. Also, we expect the function R to have a jump (or even discontinuity) at $KL(1 - \cos\theta) = 2\pi$, when negative orders of scattering [21] pop the reflectivity up. We expect conditions (18)–(20) to be broken at $p \approx 3.6$. We have no sure experimental data for $p \approx 3.6$ or larger, and in this paper we do not try to reproduce the behaviour of reflectivity at such large values of p. Therefore, we declare equations (18)–(21) as a guess for the practical case rather than a general compulsory requirement.

The intelligent estimate for the reflectivity should reproduce the asymptotic behaviour of the function R in the special cases above.

3. Fits for special cases

For applications, the most practical representation of a complicated function is the approximation with simple known functions. We wanted to approximate function R with an elementary function. We go to construct such an approximation using functions R_p and R_s mentioned above. In this section, we prepare simple approximations for these functions.

The combination of asymptotic estimate to a general fit has analogies. The famous example is Planck's formula; the combination of the formula by Rayleigh–Jean and that by Wien happened to be an exact fundamental expression. Another example is the approximate of the capacitance of the rough-surface capacitor [22]. In that paper, two independent estimates are constructed: the local height approximation and the divergent perturbative series. Then these two estimates are combined into a fit, keeping additional requirements. Several such fits give similar predictions of the capacitance. We believe that this is a methodologically correct way to treat perturbative solutions.

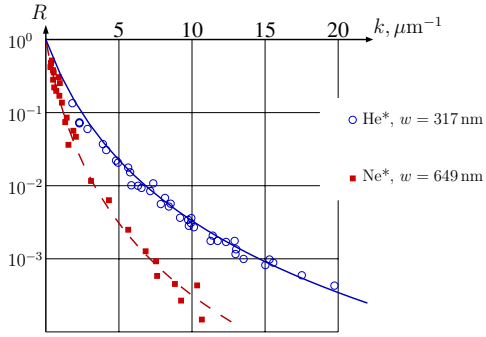

Figure 3. Fit $R_{\text{flat}}(Ksw)$ of reflectivity of the ridged mirror by (26) and (25) versus transversal wavenumber $k = K\sin\theta$ for He* ($C_4 = 8.4 \times 10^{-56}$ J m^4, $w = 317$ nm) and Ne* ($C_4 = 7 \times 10^{-56}$ J m^4, $w = 649$ nm), and experimental data in [17] (circles) and [16] (squares).

For the reflectivity of a ridged mirror, we have the approximation R_{s} of dense ridges with scaling of the van der Waals constant in [18] and the rough perturbative estimate R_{p} by equations (2)–(7) considered by [21]. None of these two estimates is expressed with an elementary function. First, we construct appropriate firs for each of these functions.

We need to exclude the function $\mathcal{E}$ (which is not elementary) from the estimate R_{p}. Instead of function $\mathcal{E}(z)$, as a solution of equation (7), we use

$$E(z) = \frac{6z^{1/4} + 5z^{2/3} + 15z}{6 + 15z^{2/3}}. \tag{22}$$

Both E and $\mathcal{E}$ are slowly increasing functions; at small values of the argument, they increase as a quarter power of the argument; at large values they increase as a cubic root of the argument. The deviations $|E(z) - \mathcal{E}(z)| < 0.02$ and $|E(z) - \mathcal{E}(z)|/E(z) < 0.02$ are small compared to the internal error of the estimate (5). After such a replacement, the function R_{p} by equation (5) becomes an elementary function; at the graphics, the initial function R_{p} practically overlaps with such an elementary-function surrogate. Therefore, below we use the same notation R_{p} for the function by (5) with substitution $\mathcal{E} = E$ using (22).

Also, we go on to use the reflectivity of a flat surface. After papers [17, 23] we expect it to be a function of single variable

$$q = Ksw. \tag{23}$$

We suggest the following fit:

$$R_{\text{flat}}(q) \approx R_{\text{q}}(q) = (1 + q)^{-4}. \tag{24}$$

The fit (24) shows a very good agreement with experimental data; the deviation does not exceed the statistical dispersion of data (figure 3). The curves for the fit R_{q} practically coincide with the curves representing R_{flat} considered by [16, 17]. The curve for He* is almost the same, as the lowest curve in figure 2; it is the same case of reflection of cold He* atoms from flat surfaces.

There is analogy between equation (24) and the asymptotic behaviour of various orders of diffraction discussed in [21], although in that paper parameter q had a little bit different meaning. The similarity becomes visible, if we treat Kw^2 as some effective period L which emulates the VWI with depth w. However, this is rather a hint, how to guess the fit, than a deduction. We have not calculated that the potential of interaction makes equation (24) exact; perhaps, such a potential can be constructed with methods of the inverse scattering problem. The calculation of such a potential and the interpretation can be a matter of an independent research.

Now we can use the fit R_q by equation (24) to simplify the estimate R_s of reflectivity of a ridged mirror. We redefine q for the ridged mirror, scaling it with factor $\sqrt{\ell/L}$. This scaling corresponds to the scaling of the van der Waals constant C_4 with factor ℓ/L, discussed by [18]. We overload the definition of q for the ridged mirror, setting

$$q = Ksw\sqrt{\ell/L}. \tag{25}$$

At $L = \ell$, this definition coincides with that by equation (23) for the flat surface.

Now we can write the rational approximation of the estimate R_s with scaling of the van der Waals constant [18] as follows:

$$R_s \approx R_q = R_q(q) = \left(1 + Ksw\sqrt{\ell/L}\right)^{-4}. \tag{26}$$

The estimate R_q and the perturbative estimate R_p by (5), (2), (3) and (22) are partial estimates which we go to combine in the next section.

4. General fit

In this section, we combine the estimates (5) and (26) into the general fit (28) below. As the large values of parameter $p = \sqrt{KL}s$, the Fresnel diffraction determines the reflection, and the general fit of reflectivity should behave as $R_p(L, \ell, K, s, w)$ by (5). At the large values of parameter $q = sKw\sqrt{\ell/L}$, the quantum reflection is important, and the fit should behave as $(1+q)^{-4}$ according to (26). We modify the fit function step by step, in order to make it to satisfy criteria.

The properties of function R discussed in section 3 limit the freedom in construction of a general fit. Here, we consider an example of such a fit. We begin with scaled estimate R_q by (26), and replace the unity in the parenthesis on the right-hand side of equation (26) to some function. This function should become unity at $p = 0$, and should force the result to behave like R_p at small values of q. The simplest choice for such a function is $R_p^{1/4}$. Unfortunately, such a replacement does not satisfy requirement (11) of section 2. At substitution $\ell = L$, the modified function should not depend on L. To satisfy equation (11), we scale the wavenumber K with a factor which becomes zero at $L = \ell$. We already have $\sqrt{\ell/L}$ in expression (25) for q; therefore we consider scaling with factor $(1-\sqrt{\ell/L})^a$, where a is a positive fitting parameter. While $\ell \ll L$, this factor is close to unity. Such an estimate can be written as

$$R_4(L, \ell, K, s, w) = \left(R_p\left(L, \ell, \left(1-\sqrt{\frac{\ell}{L}}\right)^a K, s, w\right)^{-\frac{1}{4}} + sKw\sqrt{\frac{\ell}{L}} \right)^{-4}. \tag{27}$$

The second term in the big parenthesis describes the drop of reflectivity due to the VWI. At large $p > 1$ and moderated values of q, this drop of reflectivity is already taken into account in the first perturbative term. Therefore the fit R_4 by equation (27) underestimates the reflectivity at moderate values of p and q. We should mitigate the drop of reflectivity due to the second term. We add it to the correction factor $(1 + b(1-\sqrt{\ell/L})^c p)^{-1}$, introducing two more fitting parameters, b and c. (To improve the fitting of experimental data, we could also replace p to some function of p and q, but we want our function to be simple.) The resulting fit can be written as

$$R_5(L, \ell, K, s, w) = \left(R_p\left(L, \ell, \left(1-\sqrt{\frac{\ell}{L}}\right)^a K, s, w\right)^{-\frac{1}{4}} + \frac{sKw\sqrt{\frac{\ell}{L}}}{1 + b\left(1-\sqrt{\frac{\ell}{L}}\right)^c \sqrt{KL}s} \right)^{-4}. \tag{28}$$

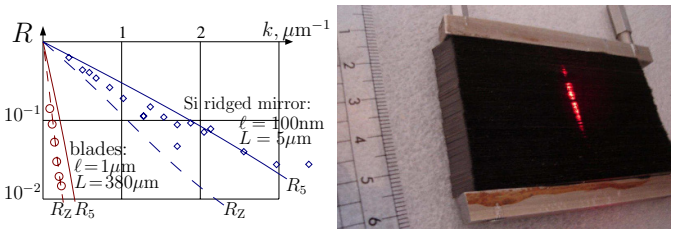

Figure 4. Reflection of photons, $K = 10\ \mu\text{m}^{-1}$. Left: reflectivity versus transversal wavenumber k. Diamonds: data with the Si sample, $L = 5\ \mu$m, $\ell = 0.1\ \mu$m. Circles: reflectivity of the stack of 130 blades, $L = 380\ \mu$m, $\ell = 1\ \mu$m. Solid curves: estimate R_5 for each case. Dashed curves: Zeno estimate for each case. Right: view of the stack of 130 blades.

The good approximation takes place at $a = 1/4, b = 3$ and $c = 4$, although the estimate is not very sensitive to the values of these fitting parameters.

For the case of flat surface ($L = \ell$), and also as for thin well-separated ridges without VWI ($q \ll 1, \ell \ll L$), function $R_5(L, \ell, K, s, w)$ does not depend on the fitting parameters at all.

For ridged surfaces, the agreement of the fit R_5 with the already published experimental data in [18, 19] is not much better than that for R_p analysed by [21]; so, we do not reproduce here the similar figures. As for the UNM sample, the deviation of the fit R_5 from the experimental data is still significant (figure 2); however, R_5 fits the data much better than the Zeno estimate R_Z by equation (1) and the perturbative estimate R_p by equation (5). Also, the fit R_5 is slightly closer to the data than the estimate R_q by equation (26).

The main advantage of fit R_5 is not the better fitting of experimental data, than various previous estimates, but its universality. The same smooth function fits the data for flat surfaces in [16, 17], the data for dense ridges (figure 2) and the data for thin well separated ridges in [18, 19].

5. Reflection of light

We expect our estimate to be valid for waves of a general kind. In this section, we compare the estimate R_5 by (28) with measurements of reflection of electromagnetic waves. However, we do not expect that some ridged mirror can reflect visible light better than a well-polished flat surface. The experiment with photons instead of atoms is important because it shows the universal character of our estimate of reflectivity, and reveals the role of defects of the ridged structure.

We have reflected the red beam of a He–Ne laser from two different ridged surfaces. First, the sample with $L = 5\ \mu$m, $\ell = 100$ nm, was used; this sample was described in [19, 21]. The solid line represents the estimate by R_5 by (28). This estimate practically coincides with the estimate R_o by (3), because $\ell \ll L$.

For visible light, the reflectivity follows our estimate until angle $\theta \approx 0.5$ rad, (figure 4(a)). At $\theta > 0.5$, the measured reflectivity becomes larger than our estimates predict (in addition, the reflectivity becomes polarization dependent); we attribute this to the reflection from the valleys between ridges which is not taken into account in our approximation. There may be many other factors which affect the reflectivity; for example, the thin ridges of Si are transparent for the red light; but anyway, our estimate predicts well the logarithm of reflectivity.

The second sample has low quality, it was assembled as stack of 130 cutter blades from a supermarket shop. (One uses such a cutter to sharpen wood pencils.) The thickness

Table 1. A range of parameters for the reflection of various waves from ridged samples.

Wave	C_4 (10^{-56} J m^4)	L (μm)	ℓ (nm)	K (nm^{-1})	θ (rad)	w (nm)
Ne*	7	30–100	40–11 000	0.95	0.0003–0.011	649
He*	8.4	0.4–5	40–100	1.26–8	0.0015–0.009	317
Light	0	5, 380	100, 1000	0.01	0.01–0.5	0

of blades determines $L = 380$ μm and we estimate the width of the edges $\ell \approx 1$ μm, although we doubt if the edges have any flat-top. The reflectivity of this sample is shown in figure 4(a) with circles. The reflectivity from such a 'bladed' mirror is lower than the estimate R_5 predicts; such deviation could be caused by the poor alignment of blades, which is seen at the grazing illumination (figure 4(b)).

For comparison, in figure 4(a) we plot also the Zeno estimate R_Z with the dashed lines, and these lines are also close to the experimental data. Metallic blades are not transparent for light; for perfectly aligned ridges, the reflectivity would be close to the estimate R_5. Defects of ridges, as well as attraction to the ridges in the case of atoms (and, perhaps, other effects), reduce the reflectivity. Therefore, the Zeno estimate (as any other function which returns values slightly smaller than the estimate R_o) shows good agreement with experiments. For better sample, the experimental data are closer to the estimate R_5, as we could expect.

The experiments with light confirm the wide area of applicability of our fit. At least this part of our experiments can easily be reproduced at any laboratory. Out fit R_5 agrees with experiments for various waves. However, it does not describe the drop of reflectivity due to defects of the ridges. It would be interesting to elaborate a procedure to characterize the defects of the ridges seen in figure 2(c) or 4(b) and to estimate how do they affect the reflectivity.

6. Limits of the approximation

We have fitted the reflection coefficient of a ridged mirror as a function of five arguments (L, ℓ, K, θ, w) with elementary function R_5, using very few fitting constants; and only one parameter, $w = \sqrt{2MC_4}\hbar$, depends on the kind of waves and the material of ridges. The fit R_5 reproduces several limiting cases, and it agrees with experimental data in a wide range of parameters (table 1). We expect that our fit has high predictive ability.

However, the approximation (28) of data in [16–19] is not much better than that by the previously published estimates. The mean-square deviation of out fit from the experimental data is about 0.04 for He* atoms, and about 0.07 for Ne* atoms. We could not significantly reduce this deviation modifying the fitting function; various functions, including fits with many fitting parameters, show similar results. We should attribute the deviation to other mechanisms. Possible sources for such deviation are as follows.

A. *Various experimental errors*. For the cases of small ratio ℓ/L ([21]) and for $\ell = L$ (flat surface, figure 3), the fitting error looks comparable to the dispersion of data.

B. The fitting errors of the partial fits R_o, R_p and R_q used in the general fit may count few per cent.

C. *Drift of the effective van der Waals constant due to oxidation of the Si surface considered in* [17]. We did not correct the data for this drift and used the same values of the effective depth of the potential $w = 649$ nm for Ne* and $w = 317$ nm for He* data.

D. *Shape of ridges and shape of the van der Waals potential*. The estimate R_p implies that the potential in the vicinity of ridges is determined by the y-coordinate and is the same

as in the case of a flat surface. For dense narrow ridges, this approximation is not so good. At small distances, the potential $U(y) = \frac{C_4}{(r_o+y)y^3}$ might provide a better approach; see [16, 24] and references therein. Also, our approximation makes no difference between trapezoidal and rectangular ridges (figure 1); the profile of ridges of the UNM sample (figures 2(b) and (c)) is very far from the trapezoidal or rectangular. At small values of ℓ, the slopes of the trapezoidal ridges [18] may affect the reflectivity.

E. *Is the potential Hermitian?* At a small distance, the VWI becomes more complicated and perhaps cannot be described as a real function of the distance. The smaller are the L and ℓ, the larger is the range of working angles, and the closer do the atoms approach to the surface. Phonons may be important for narrow ridges. The measurements at different temperatures of ridges could reveal the role of the atom–phonon interaction (see [26] and references therein).

F. *Defects of the ridges*. For the UNM sample, the fit predicts reflectivity almost twice larger than that observed. The defects of the ridges are seen in figure 2(c). Similar drop of efficiency could be caused by the poor alignment of ridges seen in figure 4(b). We do not have any model of these defects yet. We expect that the defects rather reduce the reflectivity than increase it. As the parameters of the fit are adjusted for the experimental data, our fit may slightly underestimate the reflectivity of some ideally-shaped ridged mirrors.

The mechanisms ((A)–(F)) may bring comparable contribution to the deviation of fit from the experimental data, although for some of samples the source (F) may dominate. For example, the ridges of the UNM sample are neither trapezoidal nor rectangular (figures 2(b) and (c)); they do not seem to have any 'flat top' and the size of the irregular defects seem to be comparable to their width (figure 2(c)).

The investigation of any of the mechanisms ((D)–(F)) mentioned above could be subject for the future research. In general, the fit R_5 by (28) summarizes our knowledge about reflectivity as function $R(L, \ell, K, s, w)$. It gives almost the same estimates for the reflectivity as several other fits constructed on the basis of conditions (8)–(17) and experimental data. We expect such a fit to be valid in a wide range of physical parameters.

7. Optimization on mirrors

At the manufacturing of ridged surfaces, the minimal width ℓ is determined by the precision of nano-etching machine, while L can vary in wide range. What L corresponds to the maximal reflectivity at given ℓ? In this section, we use the fit R_5 by equation (28) to estimate this optimal L.

The maximal reflectivity corresponds to the minimum of the expression in big parenthesis in (28); using equation (5) we write this expression as

$$f = \exp\left(\frac{1.68(1+0.018p^2)p}{4} + E\left(\frac{w^2}{2K\ell^3}\right)\frac{Ks\ell}{4}\right) + \frac{q}{1+b\left(1-\sqrt{\frac{\ell}{L}}\right)^c p}, \tag{29}$$

where $p = \sqrt{KL}s = \sqrt{KL}\sin(\theta)$, $q = \sqrt{\ell L}Ksw$; here, we neglect terms with $p\sqrt{\ell/L}$. In the case of efficient reflection, $p \ll 1$, $q \ll 1$, $E\left(\frac{w^2}{2K\ell^3}\right)Ks\ell \ll 1$. Expanding f by these small parameters we get

$$f \approx 1 + \frac{1.68}{4}p + q + E\left(\frac{w^2}{2K\ell^3}\right)\frac{Ks\ell}{4}. \tag{30}$$

Using definitions (2) and (25) of p and q, we get

$$f \approx 1 + \left(\frac{1.68}{4}\sqrt{KL} + Kw\sqrt{\ell/L} + E\left(\frac{w^2}{2K\ell^3}\right)\frac{K\ell}{4}\right)s. \tag{31}$$

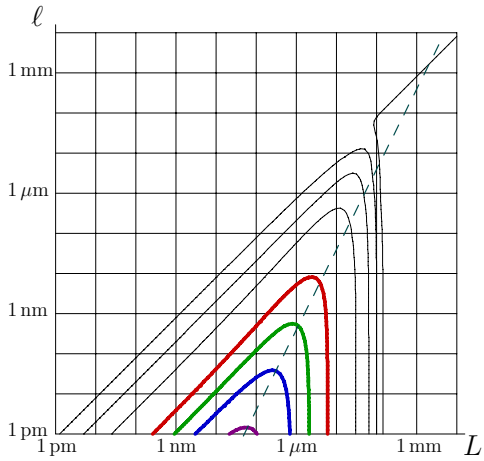

Figure 5. Lines of level $R_5 = R_5(L, \ell, K, \theta, w) = \text{const}$ at $K = 6.3\ \text{nm}^{-1}$, $w = 317$ nm, $s = 0.005$. Levels $R_5 = 0.000\,01, 0.0001, 0.001, 0.01$ (thin) and $R_5 = 0.1, 0.2, 0.3, 0.4$ (thick) are shown. (These w and K correspond to He atoms at velocity $V = 100\ \text{m s}^{-1}$.) The dashed line represents the estimate L which realizes maximal reflectivity at given ℓ by $L = 2\sqrt{K\ell w}$.

Then, the optimal $L = L_o$ can be estimated as a solution of the equations

$$\frac{\partial}{\partial L}\left(\frac{1.68}{4}\sqrt{KL} + Kw\sqrt{\ell/L}\right) = 0, \tag{32}$$

which gives

$$L_o = \frac{4}{1.68}w\sqrt{K\ell} \approx 2.38w\sqrt{K\ell} \approx 2w\sqrt{K\ell}. \tag{33}$$

We should keep only one significant figure in the last expression; after differentiating a fit, we do not expect other digits to have sense. Fortunately, the estimate (33) does not depend on the grazing angle and on parameters a, b, c of the fit (28); so, it should be even more universal than our fit.

In order to see how far is valid the estimate (33) of the optimal L, consider an example. In figure 5 we plot the estimate R_5 for He, at $V = 100\,\text{m s}^{-1}$, $s = 0.005$ in coordinates L, ℓ and draw the dashed line $L = L_o(\ell)$. We see that the estimate (33) is correct while reflectivity is larger than 0.2; the deviation becomes significant only at large values of ℓ when the reflectivity is of the order of 0.1 and lower. The most of ridged samples reported previously [18, 19] have L close to the optimal value by the estimate (33); namely for this case, the Zeno estimate R_Z by equation (1) gives values close to those by the fit R_5 by (28). Although the Zeno estimate cannot be used for optimization of ridged mirrors, it gives a correct estimate of reflectivity of a ridged mirror with optimized L. In figure 6, we plot the reflectivity as a function of L for the same case as in figure 5, for various values of width ℓ of the ridges. Each curve corresponds to the horizontal cross-section of figure 5. The maximum of reflectivity is wide; in the vicinity of optimized period L, the reflectivity is not sensitive to this parameter.

Now we reveal the role of each mechanism, Fresnel diffraction and the VWI in the reflectivity. The dashed line in figure 5 separates the domain of the Fresnel diffraction from the domain of the scaled VWI. On the left-hand side ($L < L_o$), the QR is important; on the right-hand side of this line, ($L > L_o$), the Fresnel diffraction is important. At $L \ll L_o$, the scaling of the effective van der Waals constant [18] gives the good description of the phenomenon;

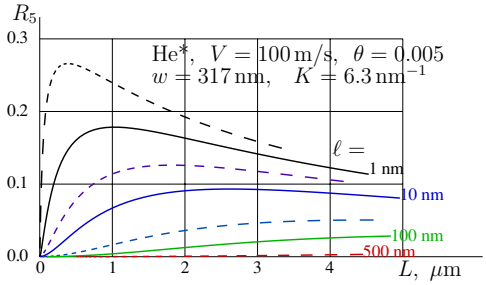

Figure 6. Reflectivity by estimate R_5 versus length L at $\theta = 0.005$ and various values $\ell = 0.1$ nm (dashed), 1 nm, 4 nm (dashed), 10 nm, 40 nm (dashed), 100 nm, 500 nm (dashed), 1000 nm for He atoms, $V = 100\,\mathrm{m\,s^{-1}}$, $K = 6.3\,\mathrm{nm^{-1}}$.

at $L \gg L_o$, the approximation of thin ridges (3) is good and the Fresnel diffraction is the main mechanism which determines the reflectivity of a ridged mirror. The intermediate region where both effects are important is a strip around the dashed line.

Normalized transversal momenta p and q are most important parameters which determine the reflectivity. For the optimized width L, these parameters have the same order of magnitude, $p \approx 2q$. Parameters p and q determine the 'loss of reflectivity' due to the Fresnel diffraction and that due to the quantum reflection, respectively. At $p > 1$, the reflectivity drops due to the Fresnel diffraction. At $q > 1$, the reflectivity drops due to the VWI. In order to have significant reflection (say, more than 10%), each parameter should be smaller than unity.

The fit R_5 also predicts the maximal width of ridges at which the ridged mirror may have a practical sense. In particular, in the case of He atoms with grazing angle 0.005, the ridges should be narrower than 100 μm. At larger values of ℓ, the maximum reflectivity takes place at $L = \ell$, i.e., the flat surface. This corresponds to the upper right side of the figure. However, at velocity $V = 100\,\mathrm{m\,s^{-1}}$ and $s = 0.005$, such a reflectivity is smaller than 10^{-4}. It would be interesting to compare such an estimate to results of numerical analysis of scattering of waves at periodic structures [27, 28]; unfortunately, many numerical algorithms become inefficient simulating scattering at grazing incidence.

In figure 5, the equi-line $R_5 = 10^{-5}$ crosses the gridline $L = 0.1$ mm twice: at $\ell \approx 20\,\mu$m and at $\ell \approx 90\,\mu$m. This means that at $\ell \approx 20\,\mu$m, the optimal $L = \ell$, i.e., the flat surface reflects atoms better than the ridged mirror does. This looks reasonable, but in figure 5, $L = 0.1$ mm corresponds to $p \approx 4$; at such values, the minus-first order of scattering [21] enhances the reflectivity; this is not taken into account in our fit. Therefore, the maximal width ℓ discussed above is a qualitative extrapolation rather than a quantitative estimate.

The minimal width is much more practical than the maximal width. For the enhancement of the range of the working grazing angles, ridges should be narrow. As the best, there should be a single-atom chain on the top of each ridge. The width of the structure cannot be smaller than the size of an atom (say, twice Bohr radius). This determines the natural limit to the minimal width ℓ of the ridges and the corresponding optimal period L, and the resulting limit of the performance of the ridged mirror.

The following improvement of atomic mirrors may involve three-dimensional structures (for example, nano-balls and/or nano-wires at thin supporting peaks) and/or other mechanisms of interaction (for example, a nano-scaled structure of magnetic dipoles). In principle, any entanglement of an atomic state to other degrees of freedom causes QR. The boundary of the domain with efficient entanglement should be sharp; the width of this boundary determines the minimal transversal wavelength $2\pi/k$, at which the waves can be efficiently reflected.

8. Asymptotic analysis of optimal L

In the previous section, the derivative of the fit R_5 by equation (28) with respect to L was used to get the estimate (33) of the optimal period L. We need to be really brave and/or to have a really good fit in order to differentiate it. However, the editors, readers and designers of the nanoscope (suggested in the next section) have no need to share our courage and enthusiasm. Therefore, in this section we use an independent asymptotic approach; we get very similar asymptotic estimate (42) below without using any fitting functions.

Consider the case of very small grazing angle, when the reflectivity is almost unity. Then we may expect each of mechanisms, VWI and Fresnel diffraction, to give additive losses to the reflectivity. That due to VWI can be estimated on the basis of the asymptotic expansion by [23] and the scaling of the van der Waals constant by [18]; in our notations, this leads to the estimate

$$R = 1 - 4q + \mathcal{O}(q^2). \tag{34}$$

This expression exactly coincides with the expansion of the fit (26). From the good agreement with experimental data (figure 2) we could expect the similarity; the exact coincidence is a gift of fortune.

The drop of reflectivity due to the Fresnel diffraction is governed by parameter p by equation (2). We need to express the first coefficient, let denote it by $-D$, of the expansion of reflectivity of ideally thin ridges with respect to p:

$$R = 1 - Dp + \mathcal{O}(p^2). \tag{35}$$

Physically, such an expansion corresponds to very small values of the grazing angle. In order to get simple expression for D, we use the analytic solution in [21]. In that paper, the solution of the paraxial wave equation is expanded by plane scattered waves; the square of norm of the residual of such solution is expressed as a quadratic polynomial with respect to amplitudes of scattered waves, and the coefficients of this polynomial are denoted as C, $-B$ (which is vector) and A (which is matrix). For calculation of the coefficient D in (35), we need to take into account only single scattered wave. This leads to the estimate of the reflectivity

$$R = C/A_{00} + \mathcal{O}(p^2) \tag{36}$$

where

$$C = \int_0^\infty \operatorname{erfc}\left(\frac{t+p}{1-\mathrm{i}}\right) \operatorname{erfc}\left(\frac{t+p}{1+\mathrm{i}}\right) \mathrm{d}t, \tag{37}$$

$$A_{00} = \int_0^\infty \operatorname{erfc}\left(\frac{t-p}{1-\mathrm{i}}\right) \operatorname{erfc}\left(\frac{t-p}{1+\mathrm{i}}\right) \mathrm{d}t, \tag{38}$$

and erfc is the complementary error function [25]. From (35), the coefficient D can be expressed as follows:

$$D = 2\left(\int_0^\infty \left|\operatorname{erfc}\left(\frac{t}{1-i}\right)\right|^2 \mathrm{d}t\right)^{-1} = 1.772\,453\,850\,905\,516\ldots. \tag{39}$$

This value is close to constant 1.68 in the fit R_o.

Assuming that the losses of reflectivity are additive, we combine the asymptotic expansions (34) and (35) and get

$$R = 1 - Dp + \mathcal{O}(p^2) - 4q + \mathcal{O}(q^2) = 1 - D\sqrt{KL}s - 4\sqrt{\ell/L}Kws + \mathcal{O}(p^2 + q^2). \tag{40}$$

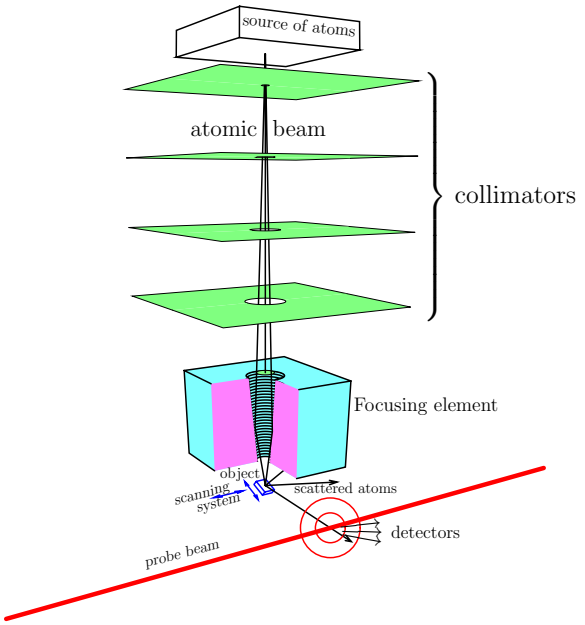

Figure 7. Scheme of the atomic nanoscope with an atomic mirror.

At the optimal L, the derivative with respect to L should be zero; this gives the equation

$$D\sqrt{KL} = 4Kw\sqrt{\ell/L} \tag{41}$$

or

$$L = \frac{4}{D}\sqrt{w^2\ell/K} \approx 2.26\sqrt{w^2\ell/K}. \tag{42}$$

For the asymptotically optimized L, $Dp = 4q$. This result is very similar to that we get from the estimate (33). The estimate (33) of the optimal period L, deduced in the previous section from the fit (28), agrees with the asymptotic analysis.

9. Nanoscope

In this section, we use the fit R_5 to estimate the maximal performance of the ridged mirrors and minimal limit of resolution of an atom optics imaging system with a ridged mirror as a focusing element (figure 7). We suggest the name 'atomic nanoscope' for such a device.

According to our fit, at ℓ of the order of 10 nm and L of the order of 2 μm, the He atoms coming to the mirror at the grazing angle $\theta = 0.005$ with velocity $V = 100$ m s^{-1} can be reflected with the efficiency of the order of 10%. Let us estimate how many atoms we can get for the non-destructive nanoscopy from a pinhole as a source of atomic beam.

The He atoms have velocity of the order of 100 m s^{-1} (considered in the examples above) at the temperature of

$$T = MV^2/k_B \approx 4.8 \text{ K}, \tag{43}$$

where k_B is the Boltzmann constant. This temperature is close to the temperature 4.22 K of He boiling at atmospheric pressure. The liquid He can be used both as a coolant and a source of atoms. While atoms have Maxwellian distribution by velocities, the fastest atoms go out

first; so, most outgoing atoms may have velocity slightly larger than we estimated, but here we care about orders of magnitude only.

Consider a nozzle as a simple pinhole of size a in a membrane of thickness b. Reasonable values can be around $a = 100$ nm, $b = 1000$ nm. Then, the flux of atoms can be estimated as

$$\Phi_0 = NVa^3/b. \tag{44}$$

The concentration N can be estimated from the equation for the pressure $P = Nk_BT$,

$$N = \frac{P}{k_BT}, \tag{45}$$

Using equation (43), we rewrite the estimate for the flux of atoms as follows:

$$\Phi_0 = \frac{a^3}{b}\frac{P}{MV}. \tag{46}$$

The only small portion of atoms reaches the focusing element; this amount can be estimated as

$$\Phi_1 = (2\alpha\theta)^2\Phi_0 \tag{47}$$

where

$$\alpha = \frac{\text{distance from the object to the focusing element}}{\text{distance from the focusing element to the source}}.$$

We can estimate $\alpha \approx 0.1$; then within the geometrical optics, the spot size $B_g = \alpha a$ would be of the order of 10 nm. The numerical aperture 2θ corresponds to the spot of size $B_w = 1/(2\theta K) \approx 15$ nm. We may expect the resulting spotsize to be of the order of $\sqrt{B_g + B_w} \approx 20$ nm.

Using equation (46), the flux of atoms which go to the focusing element can be estimated as

$$\Phi_1 = (2\alpha\theta)^2\Phi_0 = (2\alpha\theta)^2\frac{a^3}{b}\frac{P}{MV}. \tag{48}$$

For values suggested above, this counts 10^9 atoms s^{-1}. About 10% of these atoms succeed the specular reflection and reach the object. Also, about 10% of the rest can be scattered towards the probe beam; this reduces the flux of atoms until 10^7 atoms s^{-1}, which is still sufficient for the real-time bidimensional scanning of an object.

The illumination of the object with direct beam from the pinhole is not desirable; so, the mask should be located in the vicinity of the circular mirror, or may be even inside it as is shown in figure 7. An additional collimator (pinhole, not shown in the figure) may be placed in the vicinity of the object in order to block most of the atoms diffusely-scattered at the mirror. All atoms blocked by collimators should be pumped-out in order to avoid their entering the probe beam and to provide the free-travel length larger than the size of the device.

Variation of orientation of the sample and position of the probe beam should provide many options for the contrast of the resulting image, as in the case of a scanning electron microscope. The object is illuminated by the focused atomic beam of low NA; this should provide good depth of resolution and allow the non-destructive analysis of three-dimensional nano-objects.

The atoms from the pinhole are expected to be in the ground state, not in the meta-stable state used in the experiments with reflection of cold atoms. This has advantages and disadvantages. The polarizability of the ground-state atoms is lower than that of excited atoms; the effective van der Waals constant is lower and the reflectivity should be better than in the case of excited atoms. (All published data about ridged atomic mirrors refer to meta-stable

states of atoms.) We expect, for the ground-state He atoms, the grazing angle can be slightly extended, even improving the resolution.

The energy of particles in the probe beam should correspond to some resonant transition; for the ground-state atoms, it is in the vacuum-UV range. An alternative can be the excitation of scattered atoms with the electron beam. As the atoms have already interacted with the sample, we have no need to focus the probe beam into a narrow spot.

We do not specify the focal distance and the size of the device shown in figure 7. In the experiments with reflection of excited atoms [16–19], the total travel length of atoms from the source (magneto-optical trap) to the detector was of the order of metre. However, for the nano-imaging system, the length can be much smaller. This softens the requirements for the vacuum and allows us to work with a smaller focusing element. This element is the most important part of the nanoscope. The implementation of the focusing element should determine the size of the device.

The focusing element should be an ellipsoidal atomic mirror; focal points of this ellipsoid should be at the pinhole and the object. Various technologies can be used for the fabrication. Such a structure can be made with existing technologies writing the structure on photo-resist and chemical etching [29, 32, 33], but this may require to build the mirror from many precisely-aligned segments.

As an alternative, we may think about drilling of an ellipsoidal hole in a foliated material which consists of alternating narrow etching-resistant layers and the easy-etching layers. Then, the ridged mirror can be revealed with chemical etching.

There may be other options for fabrication of focusing element. The surface of the ellipsoidal-shaped well-polished hole can be filled by a layer of coiled nano-wires [31, 33]. The resulting ridged surface has no need to be flat-top shaped; the effective width is expected to be smaller than the radius of the nano-wire. The required separation L between wires can be achieved by placing several slightly thinner wires between coils of the main wire. Perhaps, the only few first loops of coils should be assembled manually; we expect that the VWI between the ellipsoid and the nano-wires will do the rest of the job of the assembling of the device. At large number of loops, the self-assembling option may be important. The estimate of the reflection coefficient for the periodic set of cylinders can be offered with expansion by scattered waves similar to that by [21]. Such analysis may be a matter for a future research.

Our estimates should be considered as argument in favour of development of technology of fabrication of profiled nano-structures.

10. Conclusions

Solid-state atomic mirrors can provide the precise focusing of atomic beams. The coefficient R of specular reflection of an atomic wave from a ridged mirror (figure 1) can be treated as a function of the period L of the ridges, their width ℓ, wavenumber K, grazing angle θ and depth w of the van der Waals potential. Properties (8)–(21) of function R strictly limit the class of functions which can be used as the general fit. We describe R_5 by (28) as an example of such a fit. We have checked it in a wide range of parameters (table 1) or ridged mirrors and also flat surfaces (figure 3). In the case of small period L of ridges, the fit gives values close to the estimate in [18] with scaling of the van der Waals constant. At $\ell \ll L$, the fit reproduces the reflectivity of a comb of narrow ridges calculated in [21].

Our fit allows us to optimize parameters of the ridged mirrors. The design formula (33) for the optimal L at given ℓ is suggested; it shows a good agreement with the fit (figure 5). Key parameters p by (2) and q by (25) carry most of the dependence of reflectivity on the parameters of the experiment; maximum reflectivity corresponds to $p \approx 2q$. On the grounding

of our estimates, we propose an atomic nanoscope (figure 7); the focusing element can be realized with a ridged surface. At $\ell \approx 10$ nm, $L \approx 2\ \mu$m, He atoms of velocity $V = 100\ \mathrm{m\ s^{-1}}$ at a grazing angle $\theta = 0.005$ rad can be reflected with the efficiency of the order of 0.1 (figure 6). At such values of the grazing angle, with wavenumber $K \approx 6\ \mathrm{nm^{-1}}$ and numerical aperture $2\theta \approx 0.01$ the scanning of an object with a spot of size of 20 nm could be achieved. The hole of diameter 100 nm can be used as a source of atoms; after all losses, about 10^7 atoms $\mathrm{s^{-1}}$ can be scattered from the object in the selected direction. The scattered atoms can be detected with an optical or electronic probe beam which has no need to be well collimated. Scanning of the object causes modulation of the luminescence of atoms in the probe beam; this modulation brings the image of the object.

Our estimates show the importance of technology for manufacturing profiled ridged surfaces. Such surfaces can be atomic mirrors. The focusing ridged atomic mirror could be made with etching of a foliated material or by coiling of a nano-wire inside a profiled hole. With such focusing elements, the atomic nanoscope suggested should become competitive with other kinds of microscopy.

Acknowledgments

A part of the experimental data was provided by F Shimizu. Also, the authors thank K Nakagawa, M Morinaga, Yu Senatsky, D Kendall, P Logofatu, K Kameta and V Balykin for valuable discussions. D Kouznetsov acknowledges M Kallistratova and S Okudaira for corrections of the text. H Oberst gratefully acknowledges support from the Japan Society for the Promotion of Science. This work was partly supported by the COE project 'Coherent Optical Science' of the Ministry of Education, Culture, Sports, Science and Technology, Japan.

References

[1] Poelsema B and Comsa G 1989 *Scattering of Thermal Energy Atoms from Disordered Surfaces (Springer Tracts in Modern Physics)* (New York: Springer)
[2] Hulpke E (ed) 1992 *Helium Atom Scattering from Surfaces* (Berlin: Springer)
[3] Balykin V, Klimov V and Letokhov V 2005 Atom nano-optics *Opt. Photon. News* **16** 44
[4] Balykin V I, Letokhov V S, Ovchinnikov Y B and Sidorov A I 1988 Quantum-state-selective mirror reflection of atoms by laser light *Phys. Rev. Lett.* **60** 2137
[5] Kasevich M, Weiss D S and Chu S 1990 Normal-incidence reflection of slow atoms from an optical evanescent wave *Opt. Lett.* **15** 607–9
[6] Oberst H, Kasashima S, Balykin V I and Shimizu F 2003 Atomic-matter-wave scanner *Phys. Rev.* A **68** 013606
[7] Saba C V, Barton P A, Boshier M G, Hughes I G, Rosenbusch P, Sauer B E and Hinds E A 1999 Reconstruction of a cold atom cloud by magnetic focusing *Phys. Rev. Lett.* **82** 468
[8] Lau D C, McLean R J, Sidorov A I, Gough D S, Koperski J, Rowlands W J, Sexton B A, Opat G I and Hannaford P 1999 Magnetic mirrors with micron-scale periodicities for slowly moving neutral atoms *J. Opt.* B **1** 371
[9] Drndić M, Zabow G, Lee C S, Thywissen J H, Johnson K S, Prentiss M and Westervelt R M 1999 Properties of microelectromagnet mirrors as reflectors of cold Rb atoms *Phys. Rev.* A **60** 4012
[10] Bertram R P, Merimeche H, Mützel M, Metcalf H, Haubrich D, Meschede D, Rosenbush P and Hinds E A 2001 Magnetic whispering-gallery mirror for atoms *Phys. Rev.* A **63** 053405
[11] Berkhout J J, Luiten O J, Setija I D, Hijmans T W, Mizusaki T and Walraven J T M 1989 Quantum reflection: focusing of hydrogen atoms with a concave mirror *Phys. Rev. Lett.* **63** 1689–92
[12] Doak R B, Grisenti R E, Rehbein S, Schmahl G, Toennies J P and Wöll C 1999 Towards realization of an atomic deBroglie microscope: helium atom focusing using Fresnel zone plates *Phys. Rev. Lett.* **83** 4229–32
[13] Godun R M, D'Arcy M B, Summy G S and Burnett K 2001 Prospects for atom interferometry *Contemp. Phys.* **42** 77–95
[14] Shimizu F and Fujita J 2002 Reflection-type hologram for atoms *Phys. Rev. Lett.* **88** 123201
[15] Pasquini T A, Shin Y, Sanner C, Saba M, Schirotzek A, Pritchard D E and Ketterle W 2004 Quantum reflection from a solid surface at normal incidence *Phys. Rev. Lett.* **93** 223201

[16] Shimizu F 2001 Specular reflection of very slow metastable neon atoms from a solid surface *Phys. Rev. Lett.* **86** 987–90
[17] Oberst H, Tashiro Y, Shimizu K and Shimizu F 2005 Quantum reflection of He* on silicon *Phys. Rev.* A **71** 052901
[18] Shimizu F and Fujita J 2002 Giant quantum reflection of neon atoms from a ridged silicon surface *J. Phys. Soc. Japan* **71** 5–8
[19] Oberst H, Kouznetsov D, Shimizu K, Fujita J and Shimizu F 2005 Fresnel diffraction mirror for an atomic wave. *Phys. Rev. Lett.* **94** 013203
[20] Kouznetsov D and Oberst H 2005 Reflection of waves from a ridged surface and the Zeno effect *Opt. Rev.* **12** 363–6
[21] Kouznetsov D and Oberst H 2005 Scattering of atomic matter waves from ridged surfaces *Phys. Rev.* A **72** 013617
[22] Bruce N C, García-Valenzuela A and Kouznetsov D 1999 Rough-surface capacitor: approximations of the capacitance with elementary functions. *J. Phys. D: Appl. Phys.* **32** 2692–702
[23] Eltschka C, Moritz M J and Friedrich H 2000 Near-threshold quantization and scattering for deep potentials with attractive wells *J. Phys. B: At. Mol. Opt. Phys.* **33** 4033–51
[24] Friedrich H, Jacoby G and Meister C G 2002 Quantum reflection by Casimir-van der Waals potential tails *Phys. Rev.* A **65** 032902
[25] Abramowitz M and Stegun I A (ed) 1972 *Handbook of Mathematical Functions* (New York: Dover)
[26] Zhang W and Walls D F 1994 Phonon-induced quantum pair correlation in the diffraction of an ultracold atomic beam by a crystalline solid surface *Phys. Rev.* A **50** 4069–76
[27] Logofatu P C, Coulombe S A, Minhas B K and McNeil J R 1999 Identity of the cross-reflection coefficients for symmetric surface-relief grating *J. Opt. Soc. Am.* A **16** 1108–14
[28] Gombert A, Bűhler C, Hoβfeld W, Mick J, Blasi B, Walze G and Nitz P 2004 A rigorous study of diffraction effects on the transmission of linear dielectric micro-reflector arrays. *J. Opt. A: Pure Appl. Opt.* **6** 952–60
[29] Chu A S, Zaidi S H and Brueck S R J 1993 Fabrication and Raman-scattering studies of one-dimensional nanometer structures in (1 1 0) silicon *Appl. Phys. Lett.* **63** 905–7
[30] Wang J J, Liu F, Deng X J, Liu X, Chen L, Sciortino P and Varghese R 2005 Monolithically integrated circular polarizers with two-layer nano-gratings fabricated by imprint lithography *J. Vac. Sci. Technol.* B **23** 3164–7
[31] Weiss P 2002 Circuitry in a nanowire: novel growth method may transform chips *Sci. News* **161** 83
[32] Lee S C and Brueck S R J 2004 Nanoscale two-positional patterning on Si(0 0 1) by large-area interferometric lithography and anisotropic wet etching *J. Vac. Technol.* B **22** 1949–52
[33] Dingreville R, Qua J and Cherkaoui M 2005 Surface free energy and its effect on the elastic behavior of nano-sized particles, wires and films *J. Mech. Phys. Solids* **53** 1827–854